—研究ノート—
Scientific Note

Gridded Data of MAGSAT Crustal Magnetic Anomalies in the Antarctic Region

Kazuo SHIBUYA[1], Yoshifumi NOGI[1] and Jun TAKENAKA[2]

南極域における地殻磁気異常の格子点データ

渋谷和雄[1]・野木義史[1]・竹中　潤[2]

要旨：MAGSAT 衛星の三成分フラックスゲート磁力計データを用いて合成された全磁力値から主磁場及び MPDF 法により得られる極域擾乱外部磁場を除去した南極域での地殻磁気異常が J. TAKENAKA *et al.* (J. Geomagn. Geoelectr., **43**, 525, 1991)によって求められている．我々は彼らの作成した 3°×3°メッシュデータをもとに，1°×1°メッシュの内挿格子点データを GMT プログラムを用いて作成した．そして，これら格子点データをワークステーション上の anonymous ftp サイトに置くことにより，利用者が自由にアクセスできるように整備した．

Abstract: Crustal magnetic anomalies in the Antarctic region were obtained by J. TAKENAKA *et al.* (J. Geomagn. Geoelectr., **43**, 525, 1991) applying the Mean Polar Disturbance Field (MPDF) method. We generated 1°×1° grid data sets from their original 3°×3° mesh data, using the GMT program. These data sets were prepared under an anonymous ftp site of the workstation at the Center for Antarctic Environment Monitoring (CAEM) of the National Institute of Polar Research (TCP/IP address: 133.57.3.2), and made accessible to users.

1. Introduction

Since launch of MAGSAT (Magnetic field Satellite; LANGEL *et al.*, 1981) on October 30, 1979 by NASA (National Aeronautics and Space Administration, USA), many scientists have studied crustal magnetic anomalies from the CHRONFIN tapes provided by GSFC (Goddard Space Flight Center). This data report deals also with the crustal magnetic anomalies derived from the CHRONFIN data set, where the MPDF (Mean Polar Disturbance Field) method (TAKENAKA *et al.*, 1991) was specially developed to reduce the effect of external disturbances which dominate in the Antarctic region. Data users can refer to TAKENAKA *et al.* (1991) for the geophysical background of data processing and reduction, and can assess the accuracy of the obtained mean anomaly value at each grid point from the associated uncertainty and the number of total intensity data used to calculate the mean anomaly value.

[1] 国立極地研究所. National Institute of Polar Research, 9-10, Kaga 1-chome, Itabashi-ku, Tokyo 173.
[2] 気象庁地震火山部. Japan Meteorological Agency, 3-4, Otemachi 1-chome, Chiyoda-ku, Tokyo 100.

2. Data Reduction to the Crustal Magnetic Anomaly

The data reduction scheme is illustrated in Fig. 1. From CHRONFIN tapes, we compiled a MAGANT data set, which contains the total intensity data synthesized from the vector magnetic fields, satellite position in geographic coordinates, and planetary magnetic activity index (K_p) at intervals of 0.5 s. In deriving the MAGANT data set, the data of the following satellite passes were discarded, when (1) the north- or east-component data showed large fluctuations, and (2) K_p indices were greater than 2_+. A total of 1790 satellite passes from November 1, 1979 to May 12, 1980 were selected in the MAGANT data set (Fig. 2).

The GSFC(12/83) model (LANGEL and ESTES, 1985) was adopted to subtract the core field of the Earth (spherical harmonics up to the order and degree 13); the data

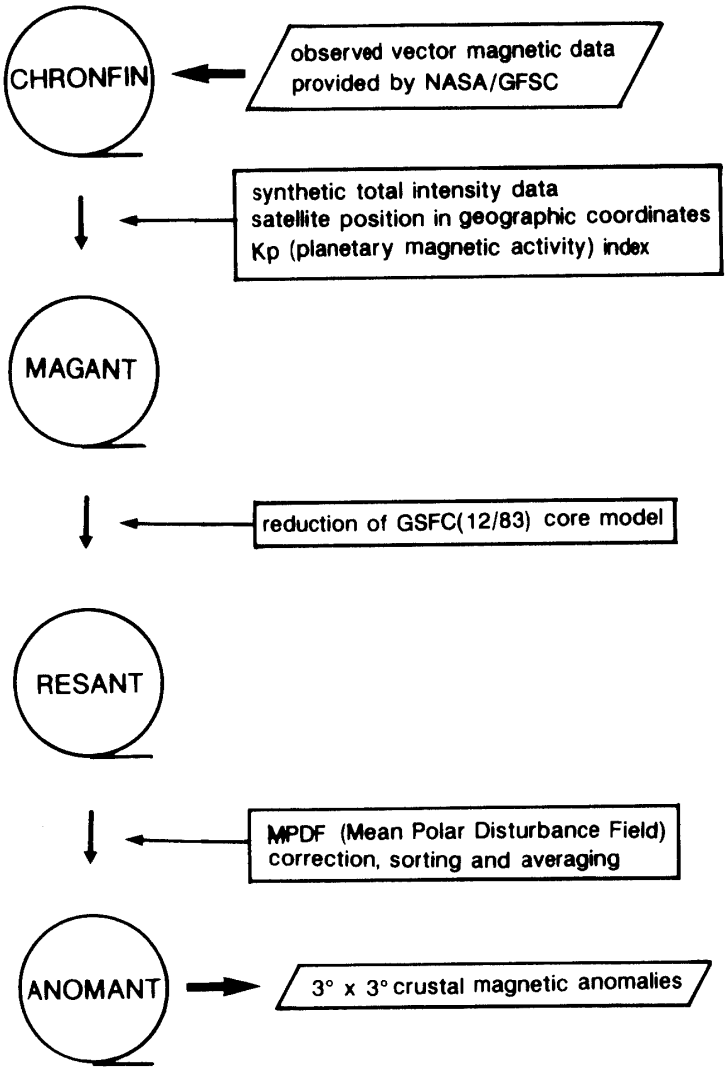

Fig. 1. Schematic data reduction procedure from the CHRONFIN data set to the ANOMANT data set.

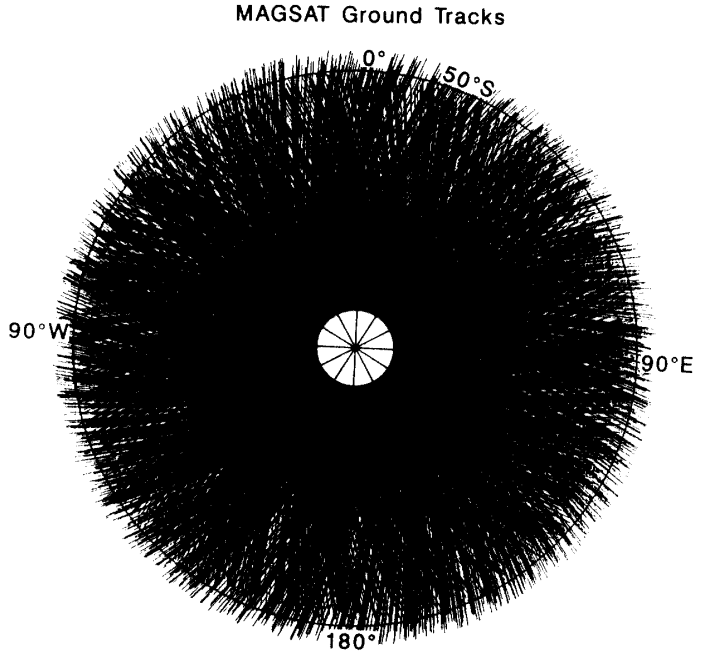

Fig. 2. Ground tracks of the MAGSAT passes selected in the RESANT data set. There is no coverage to the south of 83°S.

were reduced to the values at the epoch of 1980.0. The residual scalar data set, RESANT, can be considered as consisting of the crustal magnetic anomalies and the external disturbance field.

We assume that the observed external disturbance field shows small random fluctuations around a mean field, depending only on the geomagnetic coordinates (invariant latitude and magnetic local time (MLT)) and K_p. We divided the geomagnetic coordinate plane into sectorial areas, dividing MLT uniformly into 24 sectors with 1 hour intervals, while invariant latitude into 50 circular belts of 1° width between 40°S and 90°S. The RESANT data of each K_p index were distributed into these 1200 bins, and were averaged in each bin. Since the crustal magnetic fields are fixed to the geographic coordinates and thus vary randomly in each bin, they will be averaged out. We call the obtained average field the Mean Polar Disturbance Field (MPDF), and the MPDFs for each K_p index level, 0_0, 0_+, 1_-, 1_0, 1_+, 2_-, and 2_0 were obtained.

We subtracted each MPDF in the geomagnetic coordinate system from each subset of RESANT, whose data consists of each K_p level, then sorted the data according to geographic coordinates to obtain the ANOMANT data set. The data in the set contain the crustal magnetic anomalies observed at various altitudes (350 km -560 km), contaminated by random and small external field variations.

3. Crustal Magnetic Anomaly Data Sets

From the ANOMANT data set, areal averaging was done for the data within a $3° \times 3°$ bin to obtain the gridded crustal magnetic anomalies. There are 3 subsets

Table 1. Sample data in the DAWN3.DATA file, which are compiled from the dawnside data set of TAKENAKA et al. (1991). i and j specify grid point. ϕ and λ are geographic coordinates. ΔF and $\delta(\Delta F)$ are the obtained mean anomaly value and the associated standard deviation in nT. H and δH are the average height and the associated standard deviation in km. N and P are the number of anomaly data before averaging in the rectangular bin, and the number of satellite passes, respectively.

i	j	ϕ	λ	ΔF	$\delta(\Delta F)$	H	δH	N	P
1	1	-83.5	-178.5	-0.4	21.4	430.0	73.1	3434	297
1	2	-80.5	-178.5	-3.3	20.6	427.6	71.0	3766	211
1	3	-77.5	-178.5	-1.6	15.6	430.2	73.1	2473	92
1	4	-74.5	-178.5	-1.1	11.2	426.2	68.2	1222	33
1	5	-71.5	-178.5	-1.1	11.6	436.0	64.9	1292	29
1	6	-68.5	-178.5	0.7	11.6	435.9	76.4	1293	24
1	7	-65.5	-178.5	3.6	13.6	428.8	79.4	1461	26
1	8	-62.5	-178.5	0.5	6.0	423.6	71.0	1428	26
1	9	-59.5	-178.5	0.9	4.9	417.7	62.1	1551	22
1	10	-56.5	-178.5	-0.3	4.5	433.8	66.5	1256	20
1	11	-53.5	-178.5	-0.8	4.3	428.6	72.2	1000	16
1	12	-50.5	-178.5	1.1	3.3	428.8	78.1	902	12
1	13	-47.5	-178.5	1.8	3.1	425.2	88.2	888	13
1	14	-44.5	-178.5	0.6	3.1	452.4	90.5	992	14
1	15	-41.5	-178.5	2.2	2.2	451.5	87.3	1029	16
2	1	-83.5	-175.5	0.5	22.1	430.6	73.5	3501	301
2	2	-80.5	-175.5	-4.2	19.8	426.3	70.5	3654	211
2	3	-77.5	-175.5	-1.1	15.9	431.6	69.3	2657	96
2	4	-74.5	-175.5	-3.8	11.1	426.5	79.2	1102	36
2	5	-71.5	-175.5	0.8	13.6	431.3	61.1	1414	36
2	6	-68.5	-175.5	-1.5	6.8	435.1	68.7	1257	23
2	7	-65.5	-175.5	0.8	7.5	442.2	76.2	1245	21
2	8	-62.5	-175.5	0.6	5.9	426.4	79.5	1353	26
2	9	-59.5	-175.5	-1.6	6.7	434.8	79.1	1477	23
2	10	-56.5	-175.5	-1.8	5.2	420.6	73.5	1158	21
2	11	-53.5	-175.5	-0.9	3.9	411.9	63.6	1437	21
2	12	-50.5	-175.5	1.6	3.1	424.0	69.2	1388	21
2	13	-47.5	-175.5	2.3	2.6	439.9	67.2	1314	18
2	14	-44.5	-175.5	1.7	2.5	429.6	71.9	979	15
2	15	-41.5	-175.5	3.8	2.1	439.8	76.9	994	12
3	1	-83.5	-172.5	0.5	22.1	431.2	73.4	3518	300
3	2	-80.5	-172.5	-4.2	19.2	426.2	70.4	3697	210
3	3	-77.5	-172.5	-2.2	15.4	428.7	69.7	2281	97
3	4	-74.5	-172.5	-2.5	10.1	435.7	75.4	1359	35
3	5	-71.5	-172.5	-3.1	9.3	431.8	76.1	1264	30
3	6	-68.5	-172.5	0.4	12.2	428.4	57.7	1454	30
3	7	-65.5	-172.5	0.3	5.7	433.3	65.5	1316	19
3	8	-62.5	-172.5	0.9	5.8	447.1	78.8	1115	21
3	9	-59.5	-172.5	0.9	4.5	434.3	75.9	1320	20
3	10	-56.5	-172.5	-2.4	5.3	418.5	82.0	1056	23
3	11	-53.5	-172.5	-2.4	4.6	433.0	81.7	1506	20
3	12	-50.5	-172.5	0.0	3.4	425.6	74.7	1423	19
3	13	-47.5	-172.5	2.2	2.7	413.4	70.8	1286	19
3	14	-44.5	-172.5	1.1	2.7	407.9	62.7	1487	20
3	15	-41.5	-172.5	1.3	2.7	415.0	68.3	1377	20
4	1	-83.5	-169.5	-0.2	22.2	429.8	72.8	3516	302
4	2	-80.5	-169.5	-3.7	18.9	425.8	70.6	3767	210
4	3	-77.5	-169.5	-2.8	16.1	434.3	73.2	2118	88
4	4	-74.5	-169.5	0.0	9.2	438.2	68.6	1500	39
4	5	-71.5	-169.5	-3.0	10.0	430.7	85.8	1017	27
4	6	-68.5	-169.5	-1.6	5.7	435.0	74.0	1285	25
4	7	-65.5	-169.5	-2.5	6.7	427.7	59.5	1436	26
4	8	-62.5	-169.5	1.0	6.1	430.5	57.9	1374	22
4	9	-59.5	-169.5	1.8	5.6	435.0	77.6	1107	20
4	10	-56.5	-169.5	-0.4	4.1	450.6	78.5	1083	18
4	11	-53.5	-169.5	-2.4	3.2	438.6	75.2	1324	19
4	12	-50.5	-169.5	-0.2	3.3	427.1	82.0	1344	21
4	13	-47.5	-169.5	2.7	2.6	426.8	81.9	1380	19
4	14	-44.5	-169.5	2.6	2.4	434.5	84.3	1499	19
4	15	-41.5	-169.5	1.3	2.5	429.3	76.2	1466	19
5	1	-83.5	-166.5	-0.3	22.2	428.4	73.3	3470	300
5	2	-80.5	-166.5	-1.7	19.4	426.9	69.6	3762	212

Table 2. Similar sample data in the DUSK3.DATA file.

i	j	ϕ	λ	ΔF	$\delta(\Delta F)$	H	δH	N	P
1	1	-83.5	-178.5	0.0	0.0	450.0	0.0	0	0
1	2	-80.5	-178.5	0.0	0.0	450.0	0.0	0	0
1	3	-77.5	-178.5	2.3	22.8	398.1	48.1	400	21
1	4	-74.5	-178.5	1.6	17.6	412.5	66.8	1243	39
1	5	-71.5	-178.5	0.5	20.4	428.0	61.6	1464	37
1	6	-68.5	-178.5	-6.7	20.9	414.6	61.8	1460	30
1	7	-65.5	-178.5	-0.9	19.2	414.4	73.4	1095	21
1	8	-62.5	-178.5	-2.0	13.7	400.0	56.0	866	15
1	9	-59.5	-178.5	0.2	7.7	435.6	73.7	1269	23
1	10	-56.5	-178.5	-0.6	5.6	446.2	73.7	1814	23
1	11	-53.5	-178.5	-1.9	4.2	433.7	66.6	1539	27
1	12	-50.5	-178.5	0.3	2.8	414.2	50.0	1392	21
1	13	-47.5	-178.5	0.3	2.3	399.5	49.0	1346	19
1	14	-44.5	-178.5	-0.9	3.0	409.4	57.1	1396	18
1	15	-41.5	-178.5	1.9	3.3	411.5	56.5	1209	15
2	1	-83.5	-175.5	0.0	0.0	450.0	0.0	0	0
2	2	-80.5	-175.5	0.0	0.0	450.0	0.0	0	0
2	3	-77.5	-175.5	0.6	17.5	395.9	47.4	422	21
2	4	-74.5	-175.5	3.4	19.6	427.3	70.7	1292	37
2	5	-71.5	-175.5	-0.8	22.5	415.6	60.9	1498	33
2	6	-68.5	-175.5	-1.2	16.3	413.7	75.4	1074	22
2	7	-65.5	-175.5	-7.9	22.5	412.9	63.2	1014	23
2	8	-62.5	-175.5	-0.3	14.3	445.3	73.9	1771	24
2	9	-59.5	-175.5	1.3	5.5	429.8	63.5	1520	29
2	10	-56.5	-175.5	-2.3	2.9	404.9	47.3	1296	20
2	11	-53.5	-175.5	0.2	5.3	404.8	55.3	1350	20
2	12	-50.5	-175.5	3.4	4.4	412.7	59.9	1131	16
2	13	-47.5	-175.5	3.7	3.8	413.4	55.6	1041	17
2	14	-44.5	-175.5	2.9	2.8	409.6	55.0	1015	14
2	15	-41.5	-175.5	5.8	3.3	417.6	58.6	1102	15
3	1	-83.5	-172.5	0.0	0.0	450.0	0.0	0	0
3	2	-80.5	-172.5	0.0	0.0	450.0	0.0	0	0
3	3	-77.5	-172.5	3.0	19.3	404.1	65.1	550	24
3	4	-74.5	-172.5	-0.1	21.3	422.5	60.8	1556	39
3	5	-71.5	-172.5	-0.9	13.6	416.1	73.3	1089	28
3	6	-68.5	-172.5	-3.7	19.0	421.4	68.3	1152	28
3	7	-65.5	-172.5	-0.8	11.9	441.6	70.6	1744	28
3	8	-62.5	-172.5	3.1	6.3	407.8	47.6	1332	22
3	9	-59.5	-172.5	4.3	5.4	405.1	57.7	1283	20
3	10	-56.5	-172.5	3.3	7.9	412.6	61.8	1029	17
3	11	-53.5	-172.5	0.6	5.6	412.7	58.4	1086	16
3	12	-50.5	-172.5	2.2	4.2	420.8	62.8	1142	16
3	13	-47.5	-172.5	3.4	3.0	437.3	67.3	1222	20
3	14	-44.5	-172.5	1.9	3.0	448.7	60.6	1283	16
3	15	-41.5	-172.5	2.6	2.7	436.1	60.9	1261	17
4	1	-83.5	-169.5	0.0	0.0	450.0	0.0	0	0
4	2	-80.5	-169.5	0.0	0.0	450.0	0.0	0	0
4	3	-77.5	-169.5	2.0	21.6	420.7	63.7	729	30
4	4	-74.5	-169.5	-0.6	15.5	415.4	65.4	1394	40
4	5	-71.5	-169.5	-0.6	15.1	421.7	70.1	1149	33
4	6	-68.5	-169.5	-4.4	15.7	438.2	67.1	1652	31
4	7	-65.5	-169.5	3.3	7.9	403.4	50.2	1333	23
4	8	-62.5	-169.5	4.9	7.1	412.9	64.8	1079	19
4	9	-59.5	-169.5	2.7	5.9	414.8	61.5	1069	17
4	10	-56.5	-169.5	1.1	5.1	433.5	68.9	1178	18
4	11	-53.5	-169.5	0.5	4.9	453.2	63.4	1243	18
4	12	-50.5	-169.5	1.0	3.8	437.5	61.0	1280	19
4	13	-47.5	-169.5	3.1	3.8	428.9	53.3	1394	20
4	14	-44.5	-169.5	3.1	3.3	407.0	46.5	1497	20
4	15	-41.5	-169.5	2.9	3.5	422.5	60.1	1587	18
5	1	-83.5	-166.5	0.0	0.0	450.0	0.0	0	0
5	2	-80.5	-166.5	0.0	0.0	450.0	0.0	0	0

according to the grouping by MLT, that is, DAWN3.DATA from the dawnside (0 h -12 h MLT) data,DUSK3.DATA from the duskside (12 h-24 h MLT) data and COMB3.DATA from the combination (0 h-24 h MLT) data.

Table 3. Similar sample data in the COMB3.DATA file.

i	j	ϕ	λ	ΔF	$\delta(\Delta F)$	H	δH	N	P
1	1	-83.5	-178.5	-0.4	21.4	430.0	73.1	3434	297
1	2	-80.5	-178.5	-3.3	20.6	427.6	71.0	3766	211
1	3	-77.5	-178.5	-1.0	16.9	425.7	71.0	2873	104
1	4	-74.5	-178.5	0.3	14.8	419.3	67.8	2465	72
1	5	-71.5	-178.5	-0.2	16.9	431.7	63.3	2756	66
1	6	-68.5	-178.5	-3.2	17.6	424.6	69.9	2753	54
1	7	-65.5	-178.5	1.7	16.4	422.6	77.2	2556	47
1	8	-62.5	-178.5	-0.4	9.8	414.7	66.7	2294	41
1	9	-59.5	-178.5	0.6	6.3	425.8	68.1	2820	45
1	10	-56.5	-178.5	-0.5	5.2	441.1	71.1	3070	43
1	11	-53.5	-178.5	-1.5	4.3	431.7	68.9	2539	43
1	12	-50.5	-178.5	0.6	3.0	419.9	62.9	2294	33
1	13	-47.5	-178.5	0.9	2.7	409.7	68.5	2234	32
1	14	-44.5	-178.5	-0.3	3.1	427.2	75.8	2388	32
1	15	-41.5	-178.5	2.1	2.9	429.9	75.0	2238	31
2	1	-83.5	-175.5	0.5	22.1	430.6	73.5	3501	301
2	2	-80.5	-175.5	-4.2	19.8	426.3	70.5	3654	211
2	3	-77.5	-175.5	-0.9	16.1	426.7	67.9	3079	108
2	4	-74.5	-175.5	0.1	16.7	426.9	74.8	2394	73
2	5	-71.5	-175.5	0.0	18.7	423.2	61.5	2912	69
2	6	-68.5	-175.5	-1.4	12.1	425.3	72.6	2331	45
2	7	-65.5	-175.5	-3.1	16.6	429.0	72.1	2259	44
2	8	-62.5	-175.5	0.1	11.4	437.1	76.9	3124	50
2	9	-59.5	-175.5	-0.1	6.3	432.3	71.6	2997	52
2	10	-56.5	-175.5	-2.1	4.2	412.3	61.6	2454	41
2	11	-53.5	-175.5	-0.4	4.6	408.5	59.8	2787	41
2	12	-50.5	-175.5	2.4	3.8	419.0	65.5	2519	37
2	13	-47.5	-175.5	2.9	3.3	428.2	63.7	2355	35
2	14	-44.5	-175.5	2.3	2.7	419.4	64.6	1994	29
2	15	-41.5	-175.5	4.8	3.0	428.1	68.8	2096	27
3	1	-83.5	-172.5	0.5	22.1	431.2	73.4	3518	300
3	2	-80.5	-172.5	-4.2	19.2	426.2	70.4	3697	210
3	3	-77.5	-172.5	-1.2	16.4	423.9	69.5	2831	113
3	4	-74.5	-172.5	-1.2	17.0	428.6	68.3	2915	74
3	5	-71.5	-172.5	-2.1	11.5	424.5	75.2	2353	58
3	6	-68.5	-172.5	-1.4	15.7	425.3	62.7	2606	58
3	7	-65.5	-172.5	-0.3	9.8	438.1	68.6	3060	47
3	8	-62.5	-172.5	2.1	6.2	425.7	66.6	2447	43
3	9	-59.5	-172.5	2.6	5.3	419.9	69.1	2603	40
3	10	-56.5	-172.5	0.4	7.3	415.6	72.7	2085	40
3	11	-53.5	-172.5	-1.2	5.3	424.5	73.5	2592	36
3	12	-50.5	-172.5	1.0	3.9	423.5	69.7	2565	35
3	13	-47.5	-172.5	2.7	2.9	425.0	70.1	2508	39
3	14	-44.5	-172.5	1.5	2.9	426.8	65.0	2770	36
3	15	-41.5	-172.5	1.9	2.8	425.1	65.7	2638	37
4	1	-83.5	-169.5	-0.2	22.2	429.8	72.8	3516	302
4	2	-80.5	-169.5	-3.7	18.9	425.8	70.6	3767	210
4	3	-77.5	-169.5	-1.6	17.8	430.8	71.2	2847	111
4	4	-74.5	-169.5	-0.3	12.6	427.2	68.0	2894	79
4	5	-71.5	-169.5	-1.8	13.0	425.9	78.0	2166	60
4	6	-68.5	-169.5	-3.2	12.4	436.8	70.2	2937	56
4	7	-65.5	-169.5	0.3	7.8	416.0	56.5	2769	49
4	8	-62.5	-169.5	2.7	6.8	422.7	61.7	2453	41
4	9	-59.5	-169.5	2.2	5.8	425.0	70.9	2176	37
4	10	-56.5	-169.5	0.3	4.7	441.7	74.2	2261	36
4	11	-53.5	-169.5	-1.0	4.4	445.7	70.1	2567	37
4	12	-50.5	-169.5	0.4	3.6	432.1	72.7	2624	40
4	13	-47.5	-169.5	2.9	3.3	427.8	69.0	2774	39
4	14	-44.5	-169.5	2.8	2.8	420.8	69.5	2996	39
4	15	-41.5	-169.5	2.1	3.2	425.8	68.4	3053	37
5	1	-83.5	-166.5	-0.3	22.2	428.4	73.3	3470	300
5	2	-80.5	-166.5	-1.7	19.4	426.9	69.6	3762	212

For each data set (Tables 1–3), one data line consists of 10 elements, i and j which specify the grid point (columns 1 and 2), latitude ϕ and longitude λ which specify grid location (columns 3 and 4), obtained mean crustal magnetic anomaly ΔF

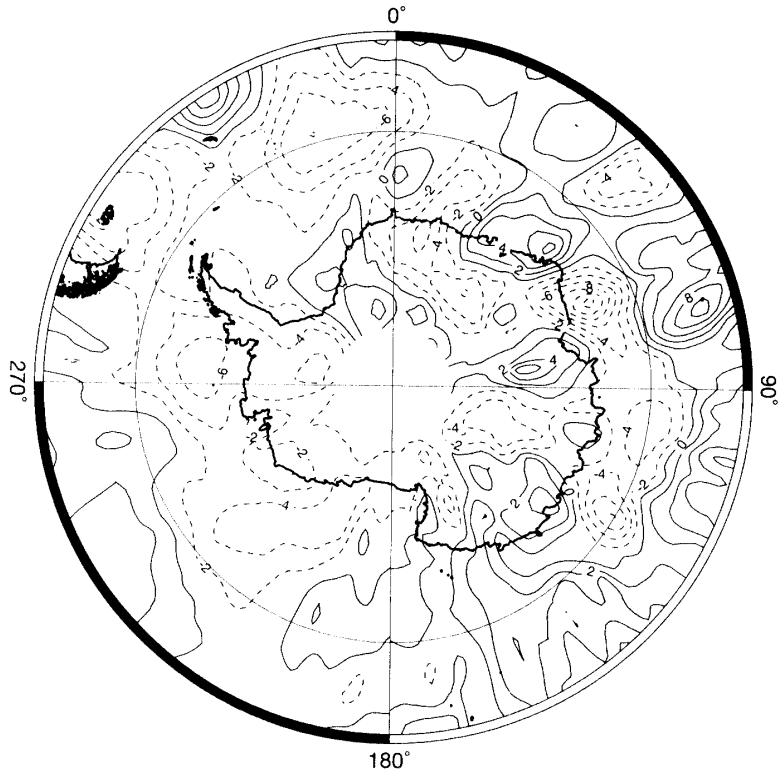

Fig. 3. Contouring of the crustal magnetic anomalies from the DAWN1.GRD using a GMT program. Solid contours are for positive areas, while dashed contours are for negative areas. Contour interval is 2 nT.

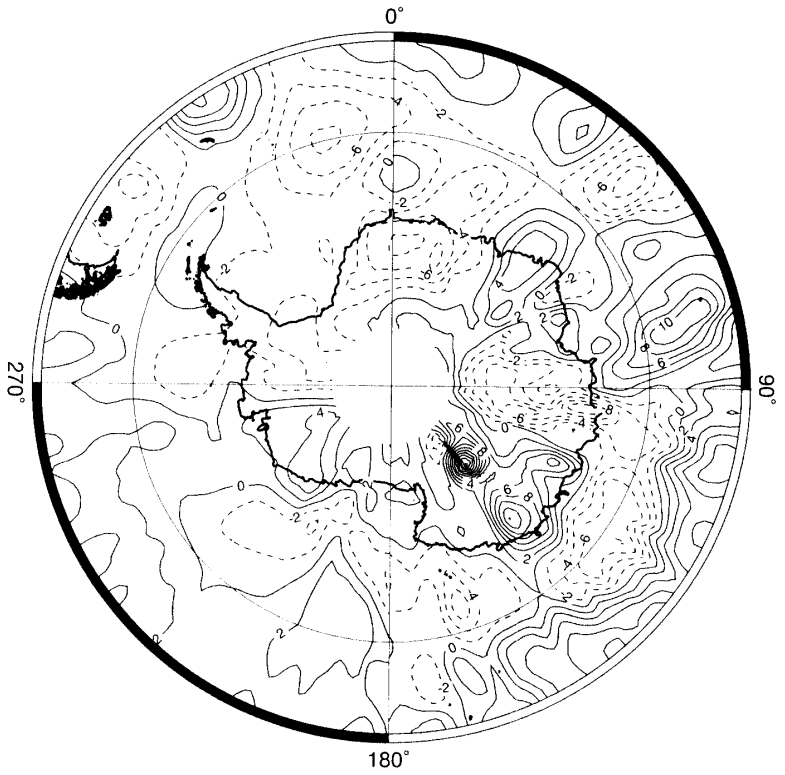

Fig. 4. Same as Fig. 3 but for DUSK1.GRD.

(column 5) and its associated standard error $\delta(\Delta F)$ (column 6), average height H of the satellite (column 7) and its associated variation δH (column 8), number of data N (column 9) and number of satellite passes P (column 10) within the corresponding bin.

4. Data Utility

Tables 1 - 3 list content samples of DAWN3.DATA, DUSK3.DATA and COMB3.DATA as explained in 3. These data sets will be prepared in a hard disk under the SUN IPX workstation of the Center for Antarctic Environment Monitoring (CAEM), National Institute of Polar Research (NIPR), and will be made accessible to users for anonymous ftp transfer (hostname geoipx.nipr.ac.jp; TCP/IP address 133.57.3.2; directory position/pub/MAGSAT). Because of limited man-

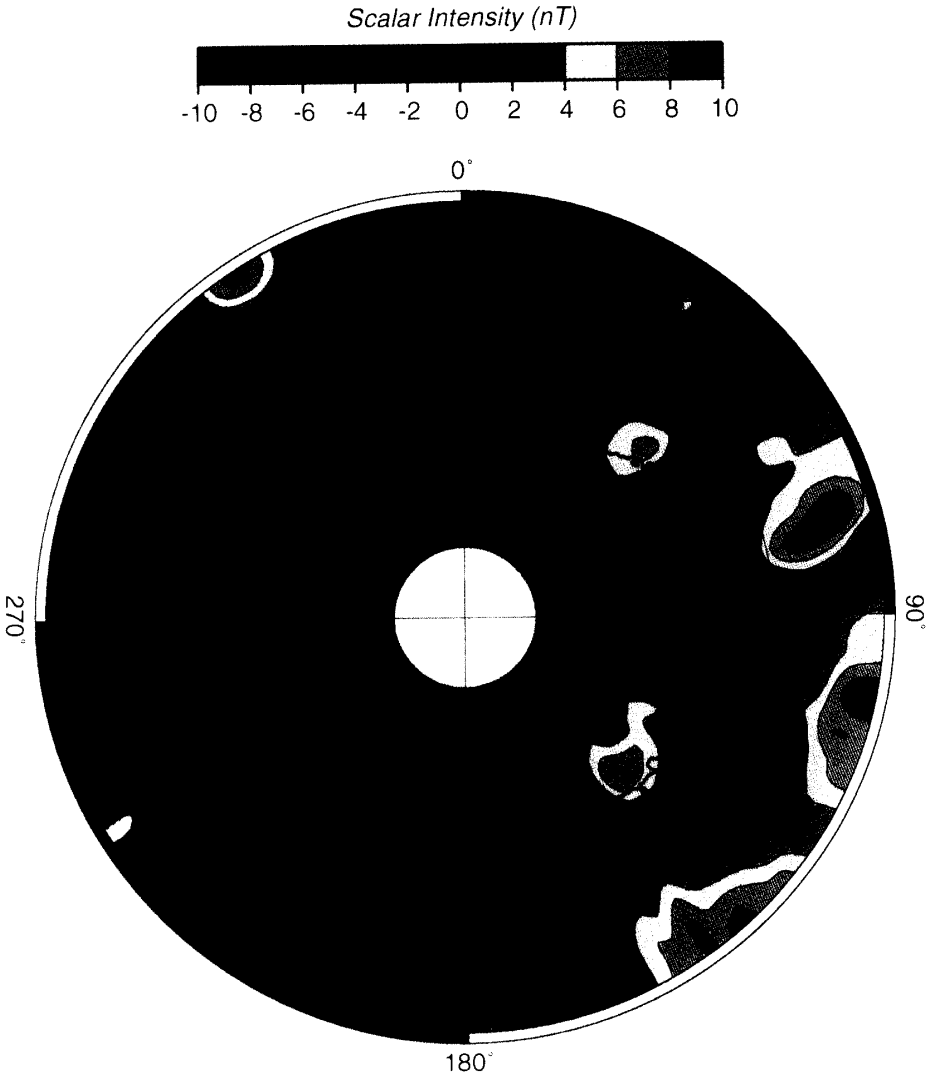

Fig. 5. Color contouring of the crustal magnetic anomalies from the COMB1.GRD using a GMT program. See scalar intensity scale.

power, we do not distribute the data on CCT media. The data retrieval procedure will be given in the read.me file of the above directory or e-mail to shibuya@nipr.ac.jp.

Fine-gridded data sets of $1^\circ \times 1^\circ$ spacing were generated from the standard $3^\circ \times 3^\circ$ grid data using a GMT program (SMITH and WESSEL, 1990; WESSEL and SMITH, 1991). They are DAWN1.DATA, DUSK1.DATA and COMB1.DATA, respectively, and are available also from the above-mentioned ftp site. These fine-gridded data are not associated with the standard deviations, satellite altitudes nor number of data, because these are interpolated from the standard $3^\circ \times 3^\circ$ data sets. One data line consists of 3 elements: grid location (longitude λ and latitude ϕ; columns 1-2) and the crustal magnetic anomaly (ΔF; column 3). Grid data sets for GMT users (DAWN1.GRD, DUSK1.GRID and COMB1.GRID) are also located in the ftp site. For reference, contoured maps of the crustal magnetic anomalies by GMT program are shown in Figs. 3-5.

Acknowledgments

The original data used in this report were those supplied from NASA in 1980-81 to the Japanese MAGSAT Team (Naoshi FUKUSHIMA, Chairman) under the Statement of Work M-43. Calculation and compilation of ANOMANT data sets was carried out on the HITAC M260H at the Information Science Center of the National Institute of Polar Research. K_p indices were made available from the World Data Center C-2 for Geomagnetism. The authors express sincere thanks to R. FUJII (Nagoya University) and M. YANAGISAWA (The University of Electro-communications) for collaboration and permission to release data.

References

LANGEL, R.A. and ESTES, R.H. (1985): The near-earth magnetic field at 1980 determined from Magsat data. J. Geophys. Res., **90**, 2495-2509.

LANGEL, R., BERBERT, J., JENNINGS, T. and HORNER, R. (1981): Magsat data processing: A report for investigators. NASA GSFC Technical Memorandum, TM82160, November.

SMITH, W.H.F. and WESSEL, P. (1990): Gridding with continuous curvature splines in tension. Geophysics, **55**, 293-305.

TAKENAKA, J., YANAGISAWA, M., FUJII, R. and SHIBUYA, K. (1991): Crustal magnetic anomalies in the Antarctic region detected by MAGSAT. J. Geomagn. Geoelectr., **43**, 525-538.

WESSEL, P. and SMITH, W.H.F. (1991): Free software helps map and display data. EOS; Trans., Am. Geophys. Union, **72**, 445-446.

(Received August 3, 1995; Revised manuscript accepted September 27, 1995)